SP-230—46

Experimental Investigation on Flexural Behavior of RC Beams Strengthened by NSM CFRP Reinforcements

by W.-T. Jung, Y.-H. Park, J.-S. Park, J.-Y. Kang, and Y.-J. You

Synopsis: This study presents the results of experiments performed on RC (Reinforced Concrete) beams strengthened with NSM(Near Surface Mounted) reinforcement. A total of 8 specimens have been tested. The specimens can be classified into EBR(Externally Bonded Reinforcement) specimens and NSM(Near Surface Mounted) reinforcements specimens. Two of NSM specimens were strengthened with 12 mechanical interlocking grooves with a width of 20 mm and spacing of 200 mm in order to prevent debonding failure of the CFRP(Carbon Fiber Reinforced Polymer) reinforcement. Experimental results revealed that NSM specimens used CFRP reinforcements more efficiently than the EBR specimens, but debonding failure between adhesive and concrete occurred. This showed that, similarly to EBR specimens, NSM specimens also required countermeasures against debonding failure. Failure mode of NSM specimens added with mechanical interlocking grooves failed by rupture of CFRP rod and strip. The measured ultimate load showed an increase of 15% compared with the common NSM specimens. The application of mechanical interlocking grooves made it possible to avoid debonding failure and to enhance strengthening performance.

Keywords: carbon fiber reinforced polymer; externally bonded CFRP reinforcements; near surface mounted CFRP reinforcements; strengthening

Woo-Tai Jung received his MS degree in Civil Engineering from Myongji University. He is a Researcher at the Structure Research Department of the Korea Institute of Construction Technology. His research interests are in the area of strengthening with FRP reinforcements of deteriorated concrete structures.

Young-Hwan Park received his MS degree and Ph.D. in Civil Engineering from Seoul National University. He is a Research Fellow at the Structure Research Department of the Korea Institute of Construction Technology.

Jong-Sup Park received his MS degree in Civil Engineering from Myongji University. He is a Senior Researcher at the Structure Research Department of the Korea Institute of Construction Technology.

Jae-Yoon Kang received his MS degree in Civil Engineering from Dongguk University. He is a Senior Researcher at the Structure Research Department of the Korea Institute of Construction Technology.

Young-Jun You received his MS degree in Civil Engineering from Yonsei University. He is a Researcher at the Structure Research Department of the Korea Institute of Construction Technology.

INTRODUCTION

Among the various strengthening techniques that have been developed and applied to strengthen deteriorated RC structures, a number of applications using FRP reinforcements have significantly increased recently. FRP reinforcements are bonded to concrete surfaces by adhesives but frequently experience debonding failure at the interface between FRP reinforcements and concrete. Most research, to date, has focused on investigating the strengthening effects and failure modes of EBR system.

The problem of premature failure of EBR system may be solved by increasing the interface between FRP and concrete. Using this principle, the NSM system has been introduced recently. The NSM system for concrete structure using steel reinforcement already began in 1940s. However, the corrosion of the steel reinforcement and the poor bonding performance of the grouting material largely impaired its application. The development of improved epoxy and the adoption of FRP reinforcement offered the opportunity to implement NSM system (Hassan and Rizkalla 2003; Täljsten and Carolin 2001). Because of their light weight, ease of installation, minimal labor costs and site constraints, high strength-to-weight ratios, and durability, FRP repair systems can provide an economically viable alternative to traditional repair systems and materials (Mirmiran et al. 2004). Rizkalla and Hassan (2002) have compared EBR and NSM system in terms of cost, including costs of materials and labor, and strengthening effect. They concluded that the NSM system was more cost-effective than the EBR system using CFRP strips.

One of failure modes in the NSM system is the debonding failure as the EBR system. Two different types of debonding failures can occur for NSM system. One is due to

spiltting of the adhesive cover as a result of high tensile stresses at the FRP-adhesive interface, and is termed “adhesive split failure”. The other is due to cracking of the concrete surrounding the adhesive, and is termed “concrete split failure”(Hassan and Rizkalla 2004). Concrete split failure is the governing debonding failure mode for NSM system because the tensile strength of the adhesive is generally greater than that of the concrete. If concrete spilt failure is delayed or prevented, the performance of the NSM system will be greatly enhanced. Epoxy keys or deformations are proposed in this study to provide the mechanical interlocking between the adhesive and the concrete.

This experimental study investigates the applicability and strengthening performances of NSM using CFRP rods and strips. For comparison, flexural tests on RC beams strengthened by EBR and by NSM have been performed. In addition, a mechanical interlocking technique has been studied to determine its effectiveness in preventing the debonding failure.

EXPERIMENTAL PROGRAM

Manufacture of specimens

A total of 8 specimens of simply supported RC beams with span of 3m have been cast. The details and cross-section of the specimens are illustrated in Fig. 1. A concrete with compressive strength of 31.3 MPa at 28 days has been used. Steel reinforcements D10(ϕ9.53mm) of SD40 have been arranged with steel ratio of 0.0041 and a layer of three D13(ϕ12.7mm) has been arranged as compression reinforcements. Shear reinforcements of D10 have been located every 10 cm in the shear zone to avoid shear failure. Table 1 summarizes the material properties used for the test beams.

Experimental parameters

Table 2 lists the experimental parameters. The control specimen, an unstrengthened specimen, has been cast to compare the strengthening performances of the various systems. SH-BOND and CPL-50-BOND, EBR specimens, have been strengthened with CFRP sheet and CFRP strip, respectively. The remaining 5 specimens were strengthened with NSM CFRP rods and CFRP strips. Among the specimens strengthened by NSM, ROD-MI-20 and PL-MI-20 included the addition of 12 mechanical interlocking grooves with a width of 20 mm and spacing of 200 mm, as shown in Fig. 2, to prevent debonding failure of the FRP reinforcement. The strengthened length of all the specimens has been fixed to 2,700 mm.

Installation of the FRP reinforcements

Fig. 3 shows the details of the strengthened cross-sections. The strengthening process of EBR specimens (SH-BOND, CPL-50-BOND) was proceeded by coating the beam with a primer after surface treatment, followed by the bonding of the CFRP sheet or strip. The strengthened beams were cured at ambient temperature for 7 days for the curing of epoxy adhesive. The process for NSM strengthening progressed by cutting the grooves at the bottom of the beams using a grinder, cleaning the debris, and embedding the CFRP rod or strip after application of the adhesive. The strengthened beams were cured for 3 days so that the epoxy adhesive achieves its design strength.

Loading and measurement methods

All specimens were subjected to 4-point bending tests to failure by means of UTM (Universal Testing Machine) with capacity of 980 kN. The loading was applied under displacement control at a speed of 0.02 mm/sec until the first 15 mm and 0.05 mm/sec from 15 mm until failure. The measurement of all test data was recorded by a static data logger and a computer at intervals of 1 second. Electrical resistance strain gauges were fixed at mid-span and L/4 to measure the strain of steel reinforcements. Strain gauges to measure the strain of concrete were located at the top, 5 cm and 10 cm away from the top on one side at mid-span. Strain gauges were also placed on the FRP reinforcement located at the bottom of the mid-span and loaded points to measure the strain according to the loading process.

EXPERIMENTAL RESULTS

Failure modes

Before cracking, all the strengthened specimens exhibited bending behavior similar to the unstrengthened specimen. This shows that the FRP reinforcement is unable to contribute to the increase of the stiffness and strength in the elastic domain. However, after cracking, the bending stiffness and strength of the strengthened specimens were seen to increase significantly until failure compared to the unstrengthened specimens.

Examining the final failure, the unstrengthened control specimen presented typical bending failure mode which proceeds by the yielding of steel reinforcement followed by compression failure of concrete. The failure of SH-BOND and CPL-50-BOND, EBR specimens, began with the separation of CFRP reinforcement and concrete at mid-span to exhibit finally brittle debonding failure (Figs. 4 and 5). Failure of CRD-NSM and NSM-PL-25, pertaining to NSM specimens, occurred through the simultaneous separation of the CFRP reinforcement and epoxy from concrete (Figs. 6 and 7). Failure of the remaining NSM specimens (NSM-PL-15, ROD-MI-20, PL-MI-20) occurred with the rupture of the FRP reinforcement(Figs. 8 and 9). Table 3 summarizes the failure modes.

Strengthening performances of EBR and NSM

Figs. 10 and 11 plot the load-deflection curves of EBR and NSM specimens, respectively. The specimens with EBR, SH-BOND and CPL-50-BOND, presented ultimate load increased by 30 to 47% compared to the unstrengthened specimen, while NSM specimens (CRD-NSM, NSM-BAR, NSM-PL-25) increased the ultimate load by 39 to 65%.

Observation of Fig. 10 reveals that even if CPL-50-BOND with relatively large cross-sectional area of CFRP reinforcement developed larger initial stiffness, premature debonding failure occurred because its bonding area is much smaller than SH-BOND. EBR specimens behaved similarly to the unstrengthened control specimen after debonding failure.

In Fig. 11, the stiffness of NSM specimens before yielding of steel reinforcement was smaller than the stiffness developed by EBR specimens. The ultimate load and yield load

are seen to increase with the cross-sectional area of NSM reinforcement.

Examining the ultimate strain of FRP summarized in Table 3, the maximum strain for EBR specimens appears to attain 30 to 50% of the ultimate strain, and 84 to 100% for NSM specimens. This proves that the NSM system is utilizing FRP reinforcement efficiently.

Mechanical interlocking

Experimental results showed that NSM specimens are exploiting the FRP reinforcement more efficiently than EBR specimens. However, they still showed debonding failure (Figs. 6 and 7). Therefore, so-called mechanical interlocking grooves (epoxy grooves) were supplemented in order to maximize the utilization of the CFRP reinforcements and prevent debonding failure (ROD-MI-20, PL-MI-20).

Figs. 12 and 13 compare the load-deflection curves developed by NSM specimens with added mechanical interlocking grooves and specimens strengthened with common NSM. As seen in Table 3, the tests performed on ROD-MI-20 and PL-MI-20 ended following the rupture of NSM CFRP rod and strip. The measured ultimate load showed an increase of 15% compared with the common NSM specimens CRD-NSM and NSM-PL-25. Consequently, it has been seen that prevention of debonding failure and improvement of strengthening performance can be achieved by adding mechanical interlocking effects to the NSM system.

CONCLUSIONS

Performance tests have been carried out on RC beams strengthened with NSM systems. The following conclusions were derived from the experimental results.

It has been seen that NSM specimens utilized the CFRP reinforcement more efficiently than the externally bonded strengthening specimens.

According to the static loading test results, the strengthening performances were improved in NSM specimens compared with EBR specimens. However, the specimens CRD-NSM and NSM-PL-25 failed by the separation of the CFRP reinforcements and epoxy adhesive from the concrete. Consequently, it is necessary to take some countermeasures to prevent debonding failure for NSM specimens.

The use of mechanical interlocking grooves made it possible to prevent debonding failure of the CFRP reinforcements and to increase the strengthening performance. Further research will investigate the influence of the width and spacing of such mechanical interlocking grooves on the flexural behavior of strengthened RC beams so as to derive their optimal dimensions.

REFERENCES

Hassan, T. and Rizkalla, S. (2003), "Investigation of Bond in Concrete Structures Strengthened with Near Surface Mounted Carbon Fiber Reinforced Polymer Strips", *Journal of Composites for Construction*, Vol 7, No. 3, pp. 248-257

Hassan, T., and Rizkalla, S. (2004), "Bond Mechanism of Near-Surface-Mounted Fiber-Reinforced Polymer Bars for Flexural Strengthening of Concrete Structures", *ACI Structural Journal*, Vol. 101, No. 6, pp. 830-839

Mirmiran, A., Shahawy, M., Nanni, A., and Karbhari, V. (2004), "Bonded Repair and Retrofit of Concrete Structures Using FRP Composites", *Recommended Construction Specifications and Process Control Manual*, *NCHRP Report 514*, Transportation Research Board

Rizkalla, S., and Hassan, T. (2002), "Effectiveness of FRP for Strengthening Concrete Bridges", *Structural Engineering International*, Vol. 12, No. 2, pp. 89-95

Täljsten, B. and Carolin, A. (2001), "Concrete Beams Strengthened with Near Surface Mounted CFRP Laminates", *Proceeding of the fifth international conference on fibre-reinforced plastics for reinforced concrete structures* (FRPRCS-5), Cambridge, UK, 16-18 July 2001, pp. 107-116

Table 1 — Summary of material properties

Material	Property	
Concrete[1)]	Compressive strength(MPa)	31.3
Tension steel reinforcement (D10) [1)]	Yield strength (MPa)	426
	Tensile strength (MPa)	562
	Diameter(mm)	9.53
	Area(cm^2)	0.7133
Compression steel reinforcement(D13) [1)]	Yield strength (MPa)	481
	Tensile strength (MPa)	608
	Diameter(mm)	12.7
	Area(cm^2)	1.267
CFRP strip[1)] (Smooth surface)	Thickness (mm)	1.4
	Tensile strength (MPa)	2452.59
	Elastic modulus (GPa)	165.49
	Ultimate strain (%)	1.48
CFRP sheet[2)] (Smooth surface)	Design thickness (mm)	0.11
	Tensile strength (MPa)	3479
	Elastic modulus (GPa)	230.3
CFRP rod [2)] (Deformed surface)	Diameter (mm)	9
	Tensile strength (MPa)	1878
	Elastic modulus (GPa)	121.42
	Ultimate strain (%)	1.55
1) from tests carried out by the authors 2) from the supplier		

Table 2 — Experimental parameters

Specimen	CFRP area (mm^2)	CFRP type	ρ_{CFRP}(%)	Strengthening method
CONTROL	–	–	–	unstrengthened
SH-BOND	26.4	Sheet	0.0489	EBR[1)]
CPL-50-BOND	70	Strip	0.1296	EBR[1)]
CRD-NSM	63.6	Rod	0.1178	NSM[2)]
NSM-PL-25	35	Strip	0.0648	NSM[2)]
NSM-PL-15	21	Strip	0.0389	NSM[2)]
ROD-MI-20	63.6	Rod	0.1178	NSM[2)]+MI[3)]
PL-MI-20	35	Strip	0.0648	NSM[2)]+MI[3)]

1) EBR: Externally Bonded Reinforcement
2) NSM : Near Surfaced Mounted Reinforcement
3) MI : Mechanical Interlocking grooves; 12ea, width : 20㎜, space : 200㎜

Table 3 — Summary of experimental results

Specimen	P_y (kN)	d_y (mm)	P_u (kN)	d_u (mm)	Increase in P_u(%)	Failure mode	ε_{uFRP}
CONTROL	46.69	12.78	56.19	71.68	-	(a)	-
SH-BOND	60.82	13.34	82.38	34.98	47	(c)	8473
CPL-50-BOND	61.04	10.52	73.24	16.00	30	(c)	4449
CRD-NSM	62.58	15.36	92.63	43.88	65	(b)	13071
NSM-PL-25	61.99	16.06	86.18	53.98	53	(b)	12350
NSM-PL-15	57.47	15.50	78.49	58.94	40	(d)	15417
ROD-MI-20	65.10	15.10	106.20	53.84	89	(d)	15710
PL-MI-20	61.83	15.68	98.72	59.8	76	(d)	15614

(a) : Steel yielding followed by crushing of concrete
(b) : Debonding of the NSM FRP reinforcement and the epoxy
(c) : Debonding of the externally bonded FRP reinforcement
(d) : Rupture of the NSM FRP reinforcement

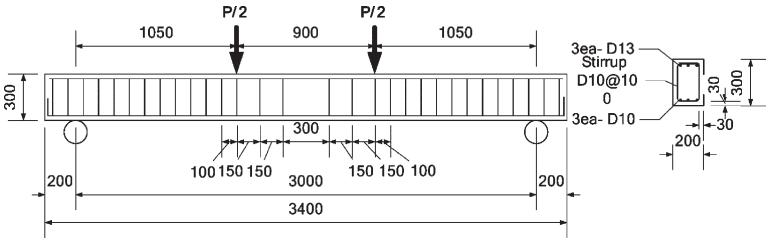

Figure 1 —Details and cross section of the specimen (mm)

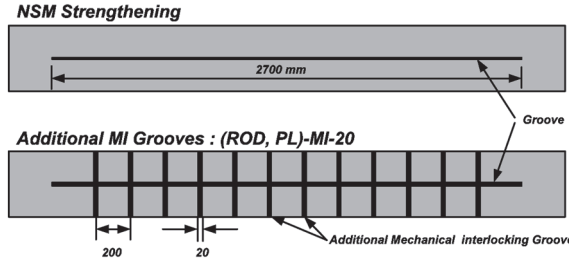

Figure 2 —Bottom schemes of RC beams strengthened with NSM reinforcement (mm)

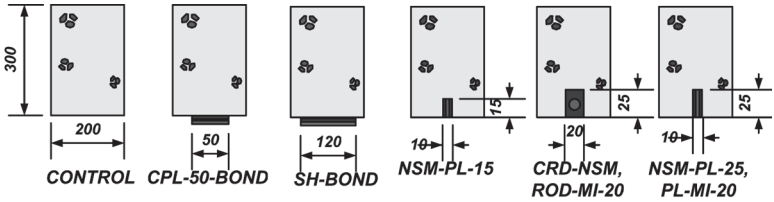

Figure 3 — FRP strengthening schemes (mm)- Cross section

Figure 4 — Failure mode (SH-BOND)

Figure 5 —Failure mode (CPL-50-BOND)

Figure 6 — Failure mode (CRD-NSM)

Figure 7 — Failure mode (NSM-PL-25)

Figure 8 — Failure mode (PL-MI-20)

Figure 9 — Failure mode (ROD-MI-20)

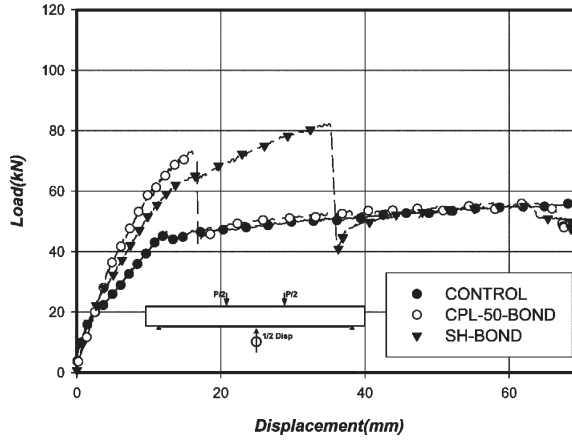

Figure 10 — Load-deflection curve: beam with EBR specimens

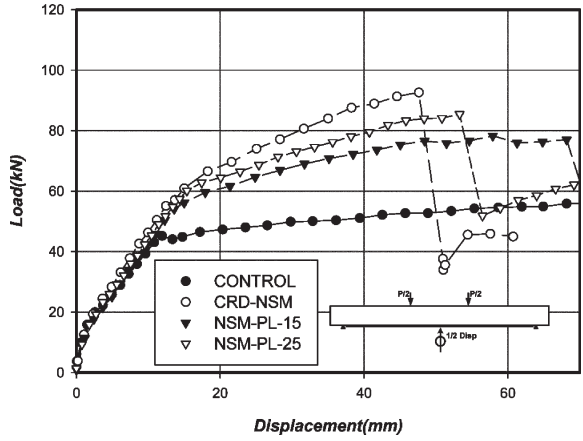

Figure 11 — Load-deflection curve: beam with NSM specimens

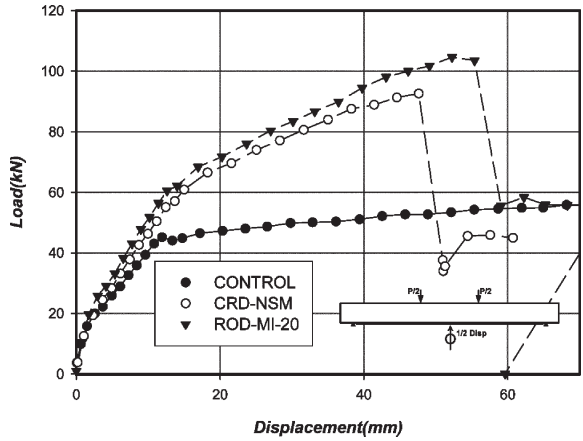

Figure 12 — Load-deflection curve: mechanical interlocking effect (CFRP rod)

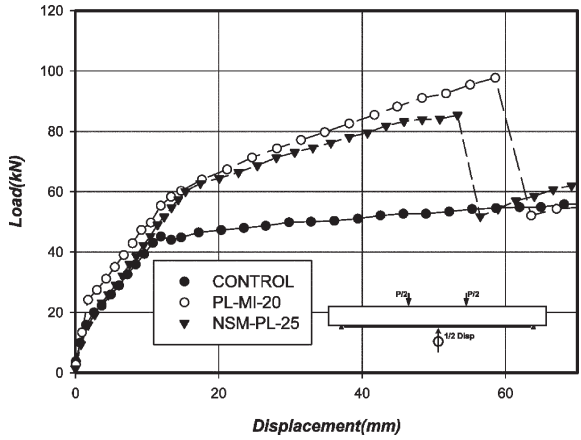

Figure 13 — Load-deflection curve: mechanical interlocking effect (CFRP strip)